Journal of Mechanical Design. Received November 30, 2019;
Accepted manuscript posted March 09, 2020. doi:10.1115/1.4046811

Design of a specialized tractor to replace draft animals in small farms

Guillermo F. Diaz Lankenau*
PhD Candidate
Global Engineering and Research Laboratory
Department of Mechanical Engineering
Massachusetts Institute of Technology
Cambridge, Massachusetts 02139
Email: diazlank@mit.edu

Amos G. Winter, V
Associate Professor
Global Engineering and Research Laboratory
Department of Mechanical Engineering
Massachusetts Institute of Technology
Cambridge, Massachusetts 02139
Email: awinter@mit.edu

This paper describes the motivation, design, and testing of a specialized farm tractor designed to replace draft animals in small farms, particularly in rural India. The proposed tractor matches the low capital cost of draft animals and has their unique ability to operate between growing crops in narrow inter-row spaces while retaining the major advantages of conventional tractors, such as low maintenance cost and reduced operator physical effort. The proposed tractor was conceived based on user needs and our implementation of a detailed terramechanics model. This tractor has a higher drawbar pull per unit mass compared to conventional tractors – a high drawbar force is needed to match the peak pull of animals, and a low mass is necessary to reduce material and vehicle costs. This quality is achieved by applying nearly the full vehicle's weight on the drive wheels, placing drive wheels in line, and locating the tillage tool between both axles. A proof-of-physics prototype of the design was instrumented to measure drawbar pull and tire slip to validate the terramechanics model and quantify traction performance. It was capable of pulling with more drawbar force per unit mass than conventional tractors and its performance can be accurately predicted by the model. During field tests on a working farm, the vehicle successfully operated in the narrow spaces between growing crops that would typically not be accessible to a low-cost, conventional small tractor. Initial farmer feedback on the design confirmed its high potential for performing farming operations.

*Address all correspondence to this author.

Nomenclature

p soil (normal) pressure
c soil cohesion
k'_c cohesion constant
γ_s soil bulk density
k'_ϕ friction constant
z depth below the surface
n depth exponent
s soil shear strength
ϕ soil friction angle
k soil shear modulus
j soil shear deformation
i slip at tire-soil interface
H tractor traction force
B tractor bulldozing force
F tractor drawbar pull
V vertical soil reaction force
w tire width
R tire outer radius at contact point
η tractive efficiency
F pulling force generated by tire
S actual forward speed of vehicle
P power delivered to wheels
D draft force
B soil bulldozing force
ψ tool angle of attack
q distance from load cell to tool
x_f distance of tractor CG to front axle
x_r distance of tractor CG to rear axle
W_T weight of the tractor

Journal of Mechanical Design. Received November 30, 2019;
Accepted manuscript posted March 09, 2020. doi:10.1115/1.4046811

θ ground slope angle
y_g distance from tractor CG to ground
y_D depth of tilling COP
x_D horz. distance from tractor rear axle to COP
α angle of draft force vector
W_I weight of the tillage tool
x_I horz. distance from rear axle to tool CG
y_I vert. distance from rear axle to tool CG

1 Introduction

A tractor designed specifically to meet the needs of small farmers in India, who would otherwise use draft animals, has the potential to create significant impact by improving farmers' economic health and India's overall food production capacity [1–3]. Small farms (< 2 ha) are common, in India the average farm size has steadily decreased from 2.28 ha in 1971 to 1.08 ha in 2016 [4], and globally (84%) of farms are less than 2 ha in size [5]. Most small farmers use a pair of bovine draft animals known as bullocks (sometimes called oxen in other countries) for all or most of their farming operations, supplemented by manual labor or a hired tractor [6, 7]. Bullocks are compact, highly maneuverable, and have a low capital cost, making them well-suited to the technical and economic constraints of small farms.

Conventional tractors, which are an icon of modern farming, are able to produce much higher farm yields than bullocks [8–11]. Farm tractors increase the capacity of each agricultural worker and enable larger, more profitable farms [12]. The Indian Agricultural Ministry estimates that farm tractors increase farm yields by 5 to 20%, reduce wasted seeds and fertilizer by 15 to 20%, and reduce farm labor by 20 to 30% [6]. However, tractors have not yet been able to replace key bullock features of maneuverability and compactness that are essential to work on a small Indian farm [13]. Tractors also have a high upfront cost that puts them out of reach of many small farmers in low income regions [14]. As a result, small-scale farmers are constrained to the slow speed of bullocks and a lack of access to suitable modern, more effective made-for-tractor tools [7, 15].

Although tractors are more expensive upfront, they are less expensive than bullocks in the long term. Fig. 1 shows the initial cost and 15 year operating costs for a bullock pair, a financed tractor, and a tractor bought upfront. A bullock pair is approximately twice as expensive as using tractors over 15 years. There are alternatives to acquiring tractors at full price up front, like financing and renting, but they are inaccessible to many farmers [14, 16, 17] and have financial drawbacks. For example, those who rent tractors forgo using the tractor for supplemental income work and risk not having access a tractor when they need one if demand is high. An ideal vehicle would retain the low upfront cost of the bullocks and the low overall cost of the tractor (e.g. the proposed vehicle in Fig. 1). Such a vehicle would have an higher value proposition than both bullocks and tractors.

To elucidate both the financial and functional requirements of a tractor specialized for small farmers, the authors interviewed stakeholders of small farming in India regarding local agricultural practices and the suitability of existing alternatives. The authors spoke with stakeholders at 12 locations in the Indian states of Maharashtra, Tamil Nadu, Gujarat, Rajasthan, Madhya Pradesh, and West Bengal. Stakeholders included farmers, research organizations, governments, and tractor manufacturers and dealers. A key observation from these visits was that small farmers used bullocks both because of their low capital cost and because of bullocks' suitability to the narrow inter-row spaces in a farm field. Bullocks have a smaller width than tractors and are more maneuverable. These characteristics allow bullocks to walk between rows of growing crops later into the season when crops are taller and wider, leaving less space between crop rows. Compared to tractors, bullocks require less space to turn at row ends, and can better traverse unfinished dirt paths leading to farm fields. These critical features of low upfront cost and ability to access narrow spaces are generally not present in commercially available small tractors. The few tractors that approach the purchase price of bullocks cannot match the bullock's maximum pulling force, a key requirement for seamlessly replacing them.

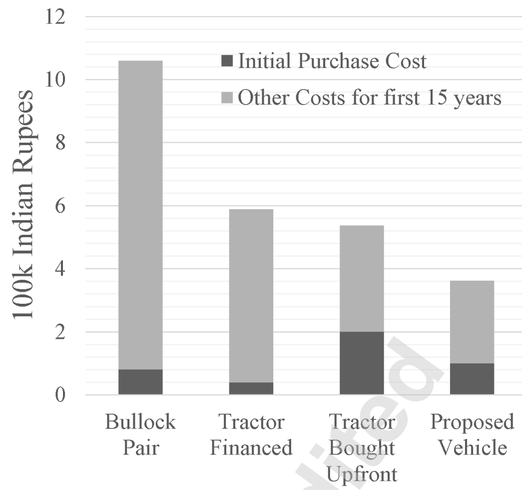

Fig. 1. CUMULATIVE COSTS OF FARMING 1 HA WITH BULLOCKS OR SMALL FARM TRACTORS. Calculations in Supplemental Material A. Values are from [7, 15, 18–21]. .

In conventional tractors, lower cost often comes at the expense of pulling force. Pulling force is related to a tractor's mass, which is correlated to purchase price. To be sold for a price comparable to bullocks (∼100k INR, as shown in Fig. 1), a tractor would likely have a mass between 350 and 500 kg given the current trends of the Indian tractor market (Fig. 2) [7, 22]. The layout of a conventional, rear-wheel-drive tractor with a mass of 350-500 kg would only produce a maximum pulling force of ∼60% of its weight (2060 N to 2940 N) in near ideal tilling conditions, and closer to ∼35% of its weight in soft soils (1200 N to 1720 N) [22–24]. This could not, under most conditions, match the maximum pulling force of a bullock pair (∼2800 N [25, 26]).

A lightweight tractor capable of replacing bullocks in small farms, and thereby improving farmers' livelihoods,

Journal of Mechanical Design. Received November 30, 2019;
Accepted manuscript posted March 09, 2020. doi:10.1115/1.4046811

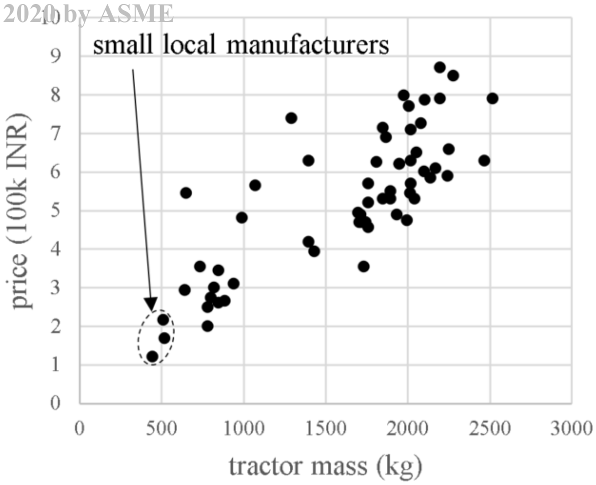

Fig. 2. RELATIONSHIP OF TRACTOR SALES PRICE TO TRACTOR MASS FOR COMMON INDIAN TRACTORS (compiled by authors, data in Supplemental Material C)

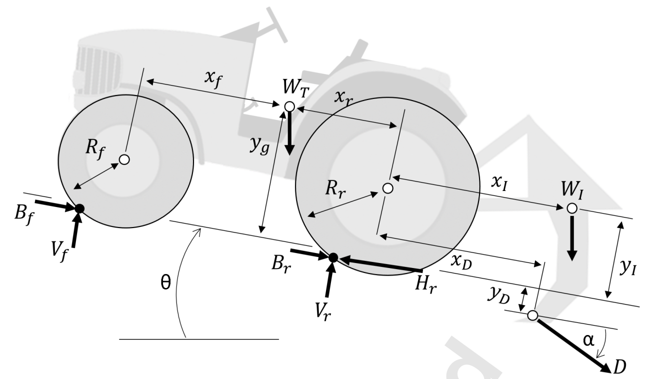

Fig. 3. FORCE FREE BODY DIAGRAM FOR A CONVENTIONAL SMALL TRACTOR. Shown are the tractor ground reaction forces (V_f,V_r,B_f,B_r, and H_r), which support the tractor weight (W_T) and tool draft (D). Key dimensions are shown, including ground slope (θ), tractor CG location (x_f, x_r, and y_g), tool CG location (x_I and y_I), tool draft center of pressure (x_D and y_D), and tool draft angle (α).

must match bullocks' pulling force, their purchase price, and their ability to enter narrow spaces. No major manufacturers currently make tractors in the bullock price range of <100k INR or with dimensions comparable to bullocks. The lightest tractors (Fig. 2) have limited pulling force (approximately 1720 N to 2940 N depending on soil conditions and actual mass) and are unable to access narrow inter-row spaces. These vehicles are made by small-volume local manufacturers near smallholder farms [27] and are not widely distributed. A manufacturer capable of making and widely distributing a low-cost tractor with the characteristics to near seamlessly supplant bullocks could likely access ∼80 million farmers currently underserved by mechanization [27, 28].

The goal of the research presented herein was to codify the parametric behavior of tractor performance, and combine this understanding with market insights to generate a tractor architecture well suited to the needs of Indian small farmers. We present our modeling approach, proposed design, and evaluation of a novel tractor.

2 Physics behind maximizing traction performance

A terramechanics-based physics model of tractors' performance derived in our prior work [29] was used to gain parametric insights on how the design of a small tractor could be manipulated to maximize drawbar force per vehicle mass. Figure 3 shows a free body diagram of the main forces acting on a farm tractor overlaid on a conventional tractor layout. For a tractor to perform an operation successfully, two main conditions based on the free body diagram must be met: (I) the vehicle must not tip over, which necessitates positive vertical ground reaction forces V_f and V_r; and (II) the tractor must achieve forward motion, which occurs when the drawbar pull force F (the sum of traction forces H and bulldozing forces B in Fig. 3) is greater than the tool draft force parallel to vehicle motion, $Dcos(\alpha)$. Additionally, when building a low-cost tractor, it is of interest to include one more condition: (III) maximize the drawbar pull to mass ratio of the tractor.

Condition (I) was evaluated by assuming the vehicle would rotate at points directly below the wheel axles and solving for the reaction forces at V_f and V_r, giving respectively:

$$V_f = \frac{1}{x_f + x_r}(W_T(x_r cos(\theta) - y_g sin(\theta)) + D(y_D + cos(\alpha) - x_D sin(\alpha)) + W_I(-x_I cos(\theta) - y_I sin(\theta))), \quad (1)$$

and

$$V_r = \frac{1}{x_f + x_r}(W_T(x_r cos(\theta) + y_g sin(\theta)) + D(-y_D + cos(\alpha) + x_D sin(\alpha)) + W_I((x_I + x_r + x_f) cos(\theta) + y_I sin(\theta))). \quad (2)$$

Where x_f is the distance from the tractor center of gravity (CG) to the front axle, x_r is the longitudinal distance from the CG to the rear axle, W_T is the weight of the tractor, θ is the ground slope angle, y_g is the distance from the CG to the ground, D is the tillage force, y_D is the depth of the tillage tool center of pressure (COP), x_D is the longitudinal distance from the tillage tool COP to the rear axle, α is the angle of the draft force vector relative to the ground slope, W_I is the weight of the implement, x_I is the longitudinal distance from the rear axle to the tillage tool CG, and y_I is the distance from the ground to the tillage tool CG.

Checking condition (II) and designing for condition (III) required an analysis that considered the physics of tire-soil interactions to calculate traction force H and tire bulldozing force B. The soil exerts a pressure on the tire (normal to the wheel perimeter) and a shear stress (tangent to wheel perimeter). All weight-bearing wheels generate a normal stress on the soil (i.e. flotation). Only braked or powered wheels generate significant shear stress on the soil (i.e. traction). The

Journal of Mechanical Design. Received November 30, 2019;
Accepted manuscript posted March 09, 2020. doi:10.1115/1.4046811

normal and shear stresses at the tire-soil interfaces were calculated from the soil's mechanical behavior.

To calculate the soil pressure p along the tire's perimeter, a common equation used in terramechanics was applied [30]:

$$p = (ck_c' + w\gamma_s k_\phi')(z/w)^n, \tag{3}$$

where c is soil cohesion, k_c' is the cohesion constant, w is tire width, γ_s is the soil bulk density, k_ϕ' is the friction constant, z is the depth below the soil surface, and n is the depth exponent (an experimental value relating penetration depth to penetration resistance).

The soil shear stress s is a function of tire-soil pressure and soil properties, and is scaled by deformation at the tire soil interface represented by term $1-e^{-j(i)/k}$ [31]:

$$s = (c + ptan(\phi))(1-e^{-j(i)/k}), \tag{4}$$

where ϕ is soil friction angle, k is shear modulus, and $j(i)$ is the shear displacement at the tire-soil interface, which is a function of tire slip i. Tire slip i is defined as $1-\frac{S}{R\omega}$, where S is the forward speed of the vehicle, while R and ω respectively are the effective radius and the angular velocity of the wheel being evaluated for slip.

To calculate the total reaction forces on the tire when contacting soil, the shear and normal stresses were integrated along the tire's casing. If the deformed tire is assumed to take the shape in Fig. 4, it can be separated into three sections: a circular arc at the front of the tire, a flat horizontal section at the bottom of the tire (the depth at which the tire total pressure matches the soil pressure), and a circular arc of the rear of the tire. Tire sinkage and deformation can therefore defined by the angles θ_c, θ_f, and θ_r in Fig. 4.

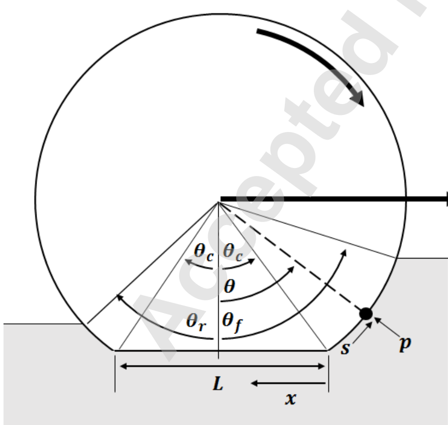

Fig. 4. PARAMETERS OF TIRE PERIMETER FOR THE CALCULATION OF FORCES AT THE TIRE-SOIL INTERFACE.

Each tire's vertical (flotation) force must satisfy Eq. 5. From this, the tire shape angles θ_c, θ_f, and θ_r can be solved for via a control strategy as shown in [32].

$$\begin{aligned} V =& wR\int_{\theta_c}^{\theta_f}[p(\theta)cos(\theta)+s(\theta,i)sin(\theta)]d\theta \\ &+ w2RP_t sin(\theta) \\ &+ wR\int_{\theta_c}^{\theta_r}[p(\theta)cos(\theta)-s(\theta,i)sin(\theta)]d\theta \end{aligned} \tag{5}$$

The traction force H and bulldozing force B can now be calculated using Eqs. 6 and 7, respectively.

$$\begin{aligned} H =& wR\int_{\theta_c}^{\theta_f}[s(\theta,i)cos(\theta)]d\theta \\ &+ w\int_0^{L(\theta_c,R)} s(\theta)dx \\ &+ wR\int_{\theta_c}^{\theta_r}[p(\theta)sin(\theta)+s(\theta,i)cos(\theta)]d\theta \end{aligned} \tag{6}$$

$$B = wR\int_{\theta_c}^{\theta_f}[-p(z)sin(\theta)]d\theta \tag{7}$$

In these expressions, w is tire width, R is tire radius, and L is the length of the tire's deformed flat section.

The drawbar pull from a single tire is the difference between its traction force H and its bulldozing force B (Fig. 3). The drawbar pull of the tractor is the sum of the drawbar pull from all of its tires. For a tractor with n number of tires, this is:

$$F = \sum_{v=1}^{n}(H_v - B_v). \tag{8}$$

The forces exerted on agricultural soil by tires affect the soil's mechanical properties (apparent in the plastic deformation in the soil in Fig. 4). Each tire pass compacts and strengthens the patch of soil it rolls over, improving the surface for trailing tires [33, 34]. Compaction is accounted for as an increase in the soil's cohesion c and bulk density γ [35]. Figure 5 is an idealized diagram demonstrating the interactions of inline drive tires on soil during loading, unloading and reloading.

Figure 6 presents a sensitivity study of drawbar pull and tractive efficiency for a conventional tractor in a common soil, loamy sand, to highlight the influence of key design parameters on small tractor performance. Tractive efficiency is the efficiency in converting power at the drive axle(s) into useful work. It is defined as $\eta = (F*S)/P$ where, η is tractive efficiency and P is power delivered to the wheel. The terramechanics model described here is highly non-linear and

Journal of Mechanical Design. Received November 30, 2019;
Accepted manuscript posted March 09, 2020. doi:10.1115/1.4046811

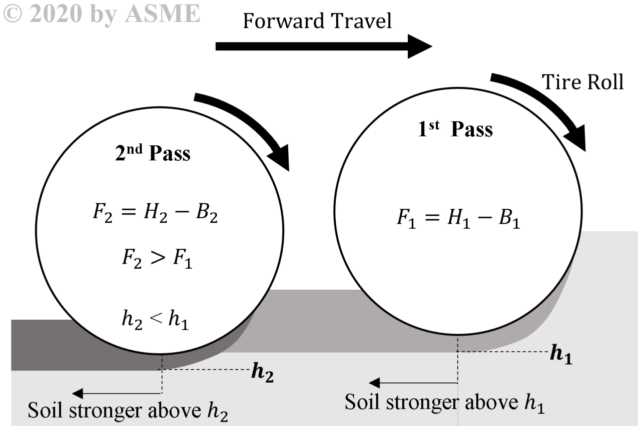

Fig. 5. ILLUSTRATION OF TIRE-SOIL INTERACTION AND MULTI-PASS EFFECT USED IN ANALYSIS. h is the depth of the compaction effect on the soil. The 2nd pass tire, which is rolling on compacted soil, can generate more drawbar pull F than it would on fresh soil since it sinks less into the soil (reducing bulldozing force B) and the soil can provide a higher shear force (increasing traction force H).

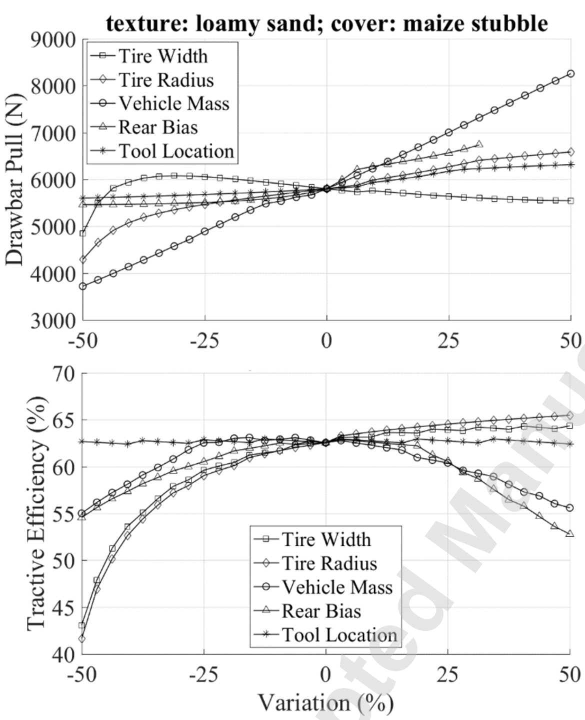

Nominal Values

Tire Width Fr.: 132mm Mass Rear Bias: 0.55
Tire Width R.: 203.2mm Tool Loc.: 0.6m after rear axle
Tire Radius: 272mm Tool Mass: 100kg
Vehicle Mass: 850kg Tool soil depth: 200mm

Fig. 6. SENSITIVITY ANALYSIS OF DRAWBAR PULL AND TRACTIVE EFFICIENCY AT 15% TIRE SLIP (A TYPICAL HEAVY TILLAGE OPERATING POINT [36]) FOR A CONVENTIONAL SMALL TRACTOR . Data were generated using the terramechanics model described in Sec. 2. Soil conditions for typical loamy sand are from [37]. In the sensitivity analysis, variables were varied ±50% from their nominal value.

depends on a large number of inputted tractor parameters. Figure 6 demonstrates that the maximum drawbar pull (net horizontal force) is approximately linearly related to the tractor mass for a large range of values.

In conventional tractors this leads to two usage trends: tractors are ballasted to increase their mass for work when a high drawbar pull is required, and high drawbar pull tools are typically mounted to the tractor behind the rear drive axle. This results in the rear axle supporting both the vertical draft forces and the tool weight, and in weight transfer from the front axle to the rear axle due to the moment generated by these forces. However, while maximum drawbar pull may increase, tractive efficiency may decrease - showing the importance of correctly matching tractor mass to tire size (and thus ground contact shape and pressure distribution). Too little weight on the tires or tires that are too wide may apply insufficient pressure to the soil, resulting in a soil that requires excessive deformation j to produce sufficient drawbar pull and therefore in power losses. Excessive weight on tires, or tires that are too thin for the required weight, will increase pressure on the soil to a detrimental degree, causing the tires to sink into the soil and exacerbating power losses to bulldozing force B.

3 Design exploration

The tractor performance model from Sec. 2 was used to identify beneficial design features to incorporate in tractors that are well suited to small Indian farmers. These features were combined to create the Bullkey tractor layout (Fig. 7). The Bullkey name is a portmanteau of *bullock* and *key* - indicating its goal of being the key to unlocking the bullock market to mechanization.

3.1 Physics-based design insights

The physics-based theory of Sec. 2 led to insights about the behavior of lightweight tractors that can improve their design and functionality for smallholder Indian farmers currently relying on bullocks as a source of draft power. The following design strategies incorporated into the Bullkey tractor (Fig. 7) maximize traction performance while incorporating or improving on many of the bullock maneuverability advantages described in Section 1.

Support the tractor mass almost exclusively on driven wheels: Only driven wheels apply a positive (drawbar pull generating) shear stress, s, on the soil. The maximum drawbar pull, F, that a tire can generate (Eqs. 6–8) is limited by soil shear strength, which depends on tire-soil pressure, p, and soil cohesion, c (term $c + p\tan(\phi)$ in Eq. 4). The soil's shear strength can be improved by increasing pressure or by increasing soil cohesion, such as via soil compaction induced by inline drive wheels (as in Fig. 5). Increasing tire-soil pressure for drive wheels is best achieved by placing more vertical load on the tires, because reducing tire width, w, or radius, R, to lower their contact area would also scale down the magnitude of traction force H in Eq. 6. It is also beneficial to limit pressure on non-driven wheels to only what is needed for stability. Idle wheels detract from the tractor's drawbar pull F since they generate no measurable traction

Journal of Mechanical Design. Received November 30, 2019;
Accepted manuscript posted March 09, 2020. doi:10.1115/1.4046811

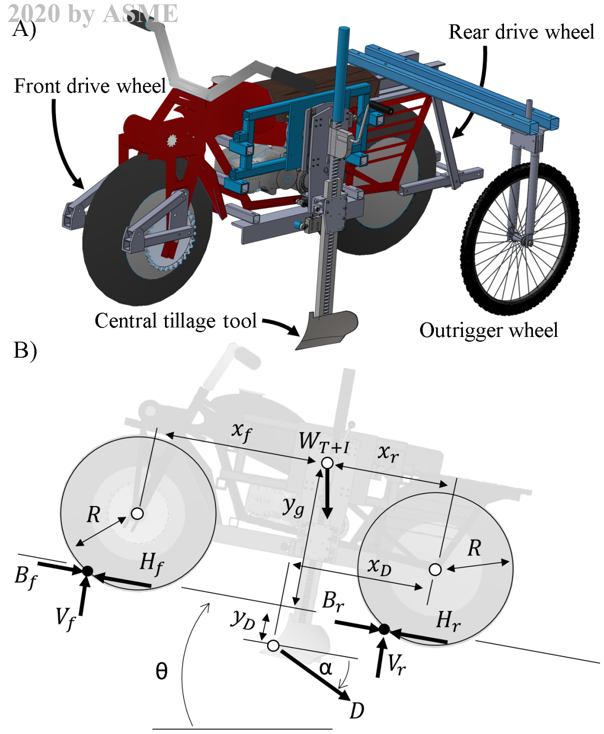

Fig. 7. (A) ISOMETRIC VIEW WITH LABELED SOIL ENGAGING COMPONENTS AND (B) FORCE FREE BODY DIAGRAM FOR BULLKEY TRACTOR.

force H (since $s = 0$) and can still generate a significant bulldozing force B which increases with applied tire-soil pressure p (Eq. 7).

Shifting weight towards the driven tires is fundamental to achieving a high drawbar pull to mass ratio. A pneumatic agricultural tire can generally generate as drawbar pull no more than 80% of the vertical load it supports [23,24], and a conventional tractor design has 50 to 80% of its total mass on its driven rear wheels [29]. Shifting more weight to the rear wheels in this layout would increase the risk of upending the tractor and reduce vehicle safety. A conventional tractor is therefore nominally able to pull up to 64% of its operating weight (even less if considering the detrimental bulldozing forces from idle wheels) in near ideal conditions, and much less in non-ideal conditions. Changing the layout to support all of the mass on the drive wheels should increase the maximum pull capacity to 80% of the vehicle's operating weight. If a tractor layout must use additional idle wheels for stability, they should be designed so that stability can be achieved while only lightly loading the idle wheels – therefore limiting the detracting opposing force they can generate and maximizing the mass supported by drive wheels.

Match tire ground pressure to required soil shear stress by operating between 10% and 25% tire slip: A tire slip of 10 to 25% has been found to be an efficient compromise between energy losses to soil shear deformation j (which is a function of tire slip i) and to soil bulldozing B [24,31,35]. A well designed tractor should have its mass and tires sized appropriately to reach its desired drawbar pull F in that tire slip range. To increase the drawbar pull generating traction force H, one must increase the applied soil shear stress s, which increases with i (Eq. 4), or increase the tire contact area (term wR in Eq. 6). Some soil shear deformation must always exist at the tire-soil interface to generate a traction force H. Reducing tire-soil slip while maintaining constant applied shear stress requires increasing the soil pressure, p, which is typically done by adding ballast to the tractor. However, increasing pressure also results in a larger tire bulldozing force B (Eq. 7), which is detrimental to drawbar pull F (Eq. 8). If instead, ground pressure is adjusted by changing tire size (i.e. contact area), the wR term will be affected in both H (Eq. 6) and B (Eq. 7), causing them both to either increase or decrease simultaneously. Therefore, an all encompassing design rule cannot be given but it is recommended to use the model from Sec. 2 to select tire sizes and a weight distribution that generate sufficient drawbar pull while staying in the desirable tire slip range.

Use inline drive wheels with similar vertical loads: Compared to side-by-side wheels, inline drive wheels increase tractor drawbar pull and efficiency because the rear drive wheel operates on soil that has become stronger (higher cohesion, c, and bulk density, γ_s) after being compacted by the front drive wheel [35,38]. In conventional tractors the front drive wheels are much smaller and lightly loaded compared to their rear side-by-side drive wheels – so the front wheels do not strengthen the soil significantly for the rear drive wheels. In agriculture, soil compaction is often considered undesirable because it hinders crop growth. However, inline drive wheels leverage a technique known as "controlled traffic", in which one patch of soil is driven over multiple times rather than driving over more areas of soil only once. This method takes advantage of the fact that if all tire passes are equivalent, compaction will be highest after the first pass and much lower for subsequent passes [33,39]. This method is less detrimental to crop yields and has been proven in farm fields across the world [40–43].

Add a mount for high drawbar tools between both driven axles: Adding a mount for high drawbar tillage tools between the front and rear axles uses the downward forces from tillage ($D * sin(\alpha)$) to increase the vertical loading on both the front and rear wheels, respectively V_f and V_R (Fig. 7). This results in higher soil-tire pressure, p, and thus higher soil shear strength (represented by $c + ptan(\phi)$ in Eq. 4). If both axles are driven, this produces a higher maximum traction force H at both drive tires and increases the tractor's maximum drawbar pull F (Eqs. 6) and 8.

Additionally, the central mount improves steering authority and stability by firmly planting both wheels on the ground, which allows the operator to safely operate the proposed tractor design near its performance limits. In contrast, the draft force, D, in the conventional tractor design (Fig. 3) causes the front wheels to become unweighted; even though the horizontal draft component, $Dcos(\alpha)$, is typically larger than the vertical component, $Dsin(\alpha)$, it exerts a torque over a much shorter moment arm (y_D vs. x_D). This unweighting of the front wheels can cause the vehicle to upend (i.e. tip over backwards) and severely injure the operator [29,44,45],

Journal of Mechanical Design. Received November 30, 2019;
Accepted manuscript posted March 09, 2020. doi:10.1115/1.4046811

and limits the operator's confidence when operating the tractor near its performance limits. In India, tractors account for over 25% of farming accidents and the upending of tractors is a common cause of serious injury [46]. This risk is mitigated by the added stability of mounting the drawbar tool between the front and rear axles.

3.2 Comparison of tractor layouts

Bullkey was designed by combining the strategies discussed in Sec. 3.1 resulting from physics modeling with insights gathered from farmer interviews, while utilizing advantageous characteristics of existing small tractor designs. Major needs of Indian small farmers are unmet by existing designs, including the ability to enter narrow (<70 cm) inter-row spaces like bullocks can, and achieving a purchase price comparable to bullocks (∼100k INR) while generating sufficient drawbar pull. A successful design should meet these needs and also account for other important considerations farmers use when evaluating tractors, like soil compaction and ease of operation. Additionally, the design must maintain desirable features of existing tractors relative to bullocks, such as reduced ownership costs, reduced drudgery, and improved farming productivity [6, 7, 28]. The analysis in this section shows that Indian small farmer needs could be better met by a novel tractor layout – particularly with respect to the location of drive wheels and the location of tillage tools.

Possible tractor layouts (Fig. 8) were selected for evaluation with respect to user needs because they are either currently popular in India (layouts A and B), have been well adopted in other countries by farms smaller than their national average (layout C) [29], or include the features identified as desirable for the Bullkey design (layout D). These layouts have distinct configurations: (A) is a conventional small farm tractor with side-by-side steering idle wheels on the front axle, side-by-side drive wheels on the rear axle, and tools behind the rear axle, (B) is a tricycle tractor similar to the conventional tractor layout but with a single front idle wheel, and (C) has a design similar to a conventional tractor but with tools ahead of the rear axle. The proposed Bullkey layout, (D), has inline drive wheels and tillage tools between the front and rear drive wheels.

Tool location impacts user comfort and safety, along with the tractor's drawbar pull capability. Placing the tool behind the rear axle, as in layouts (A) and (B), improves comfort by keeping soil detritus away from the driver during tillage and, more importantly, improves drawbar pull by transferring weight to the driven rear axle during tillage. However, this weight transfer is also detrimental to comfort and safety, as it unweights the front wheels, resulting in loss of steering authority or, ultimately, in upending the tractor. Placing the tool between the front and rear axles, as in layouts (C) and (D), improves comfort and safety by placing the tool's action near the farmer's driving line of sight and eliminating the risk of upending the tractor.

Layout (D) is singular in its ability to enter narrow spaces. Layouts (A), (B), and (C) are limited by their side-by-side drive wheels, which prevent them from straddling crop rows taller than their low ground clearance. In the case

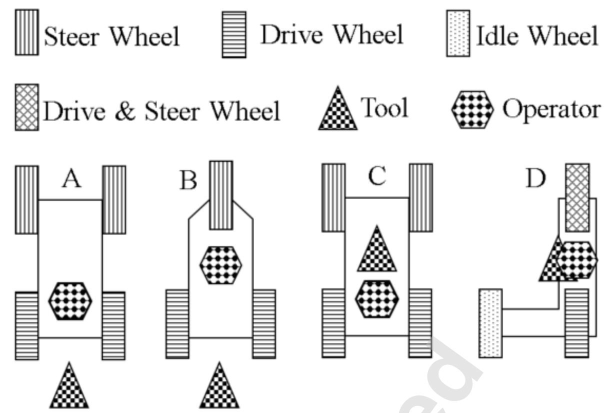

Fig. 8. TRACTOR LAYOUTS CONSIDERED FOR BULLKEY. A and B are typical small tractor layouts in India. C is an alternative vintage design that was considered. D is the chosen Bullkey layout.

of (B), the situation is worsened by the front wheel requiring a third travel lane – meaning the rows must be widened to accommodate the full vehicle in a single inter-row space or the vehicle must straddle two rows of crop. In these layouts, the major mass components – engine, transmission, and operator – are between, not in line, with the drive wheels. As such, for a vehicle of this configuration to straddle crops, a large amount of mass would have to be elevated above the crop height. In tall crops, this is deleterious to the vehicle's stability and would limit its ability to use ground engaging tools. The inline drive wheels configuration of Bullkey, layout (D), places all the major mass components in line with the drive wheels. This narrow packaging, allows access to inter-row lanes and maintains a low center of mass. Since the outrigger wheel does not generate traction or provide steering, it does not need to bear much weight and can be attached via a simple high ground clearance extension arm from the main tractor frame (Fig.7A). This allows the outrigger arm to straddle tall crops and the tractor to generate a single compaction lane (under its drive wheels).

The side-by-side drive wheel configuration in layouts (A), (B) and (C) allows for differential steering, which can be an advantage in some situations. Differential steering is the simultaneous application of different torques on each of two side-by-side drive wheels, which generates a moment on the tractor body and causes it to rotate in yaw. Differential steering can reduce the tractor's turning radius and enables the driver to maintain some control even when the steering authority of the front wheel is low (e.g., when the front wheels are unweighted). This could be replicated in (D) by a differential drive-line and steering system that allows the rear tire to be completely braked (i.e. stopped) while the front wheel is turned 90° and driven, therefore pivoting the whole vehicle around the rear tire's contact patch.

The novel layout, (D), was selected for Bullkey because it combines the drawbar pull advantages of weight transfer of (A) and (B) with the improved safety and comfort of (C). Additionally, Bullkey has a unique ability to operate in narrow spaces. The advantages of Bullkey, both in terms of draw-

Journal of Mechanical Design. Received November 30, 2019;
Accepted manuscript posted March 09, 2020. doi:10.1115/1.4046811

		Tractor Layout			
Beneficial Design Features	**User Need Met**	A	B	C	D
Weight transfer during tillage improves drawbar pull	drawbar pull	✓	✓		✓
Weight transfer during tillage improves steering authority	safety, comfort			✓	✓
Safe to operate near tillage force limits (will not upend)	safety, drawbar pull			✓	✓
Tillage tool is near farmer's driving line of sight	comfort, ease-of-use			✓	✓
All drive tires are in a single lane with farmer and tool	narrow, low soil compaction				✓

Table 1. OCCURRENCE OF DESIRABLE DESIGN CHARACTERISTICS IN EVALUATED TRACTOR LAYOUTS OF FIG. 8

bar pull and usability, are significant (Table 1) and allow it to meet the needs of small farmers in India elucidated in Sec. 1. The inline drive wheels allow Bullkey to enter narrow spaces currently only accessible to bullocks. The combination of the wheel placement and a central tool location improves the vehicle's drawbar pull per unit mass. Thus, the Bullkey design meets the required drawbar pull with a lower overall mass, lowering the purchase price for the user relative to a conventional tractor that can produce equivalent drawbar pull. Bullkey also meets the farmers' needs for improved comfort and safety by providing improved visibility of the tillage tool and eliminating the risk of upending the tractor during tillage. Additionally, soil compaction, which is detrimental to crop growth, is reduced by limiting the vehicle to a single compaction lane. Bullkey (Fig. 7) is thus uniquely capable of providing the benefits of both a pair of bullocks and a tractor.

3.3 Predicted performance

To demonstrate the relative performance advantages of Bullkey, its predicted drawbar force (using the Sec. 2 model) was compared to that of an equal mass tractor and a pair of bullocks. The mass of the modeled Bullkey and conventional tractor was set to 500 kg because market trends of cost-to-mass ratio suggest that a tractor with a cost comparable to a pair of bullocks would have a mass 500 kg or less (Fig. 2). Dimensions of the conventional tractor, except for mass, are the same as on the Mahindra Yuvraj (Yuvraj NXT 215 by Mahindra Tractors, India [47]), a popular small tractor in India. The Bullkey dimensions are those of the prototype vehicle described in detail in Sec. 4. Dimensions for both vehicles are shown in Table 2.

The pulling force of a pair of bullocks was calculated for comparison with these tractors. The bullocks' pulling force has two values, a steady pull and a maximum pull. The steady, sustained pull is about 15% of the animals' combined weight (each bullock has a mass of $\sim$300 kg [48]), while the maximum pull can be as much as 50% of the animals' combined weight [26,49]. The maximum pull plays a critical role – it allows the animals to briefly pull a tillage tool through a harder patch of soil. A tractor that cannot reach an equivalent maximum pull would become stuck in similar situations and require a decrease in drawbar pull (by reducing tool depth) to proceed. Minimizing the unplanned depth adjustments during operations improves the quality of the work and reduces

Tractor Layout	Conventional	Bullkey
Vehicle Mass (kg)	500	500
Rider Mass (kg)	60	60
Weight Front/Rear (%)	45/55	50/50
Wheelbase (m)	1.5	1.3
Tool Horz. from CG (m)	-1.5	0
Plow depth (m)	0.13	0.13
Tire sidewall height (m)	0.085	0.165
Tire diameter (m)	0.72	0.64
Tire width (m)	0.2	0.2
Tire Pressure (psi)	8.7	8.7

Table 2. PARAMETERS FOR A CONVENTIONAL TRACTOR AND THE BULLKEY COMPARED IN FIGURE 9.

drudgery. Therefore, it is valuable to have Bullkey match the maximum pulling force of bullocks to negate the need for depth adjustments in any tillage situations where the bullocks could pull through.

The model predicted that Bullkey can exceed the maximum pull of bullocks over a significantly wider range of soil conditions than conventional tractors can (Fig. 9). This translates to improved usability of Bullkey over other light tractors by reducing the likelihood of the vehicle being bogged down during tillage.

4 Proof-of-concept vehicle design

A prototype vehicle was built to validate the Bullkey concept and evaluate the model of tractor traction performance that was used to design it (Fig. 10). The prototype incorporates key Bullkey design features, including: supporting nearly all the vehicle's mass on its two inline drive wheels, incorporating a centrally mounted tillage tool, and incorporating a lightly loaded outrigger wheel that can straddle rows of growing crop. The prototype was built on a Rokon Scout motorcycle (Scout by Rokon International Inc., New Hampshire [50]), which is an all-wheel-drive, two-

Journal of Mechanical Design. Received November 30, 2019;
Accepted manuscript posted March 09, 2020. doi:10.1115/1.4046811

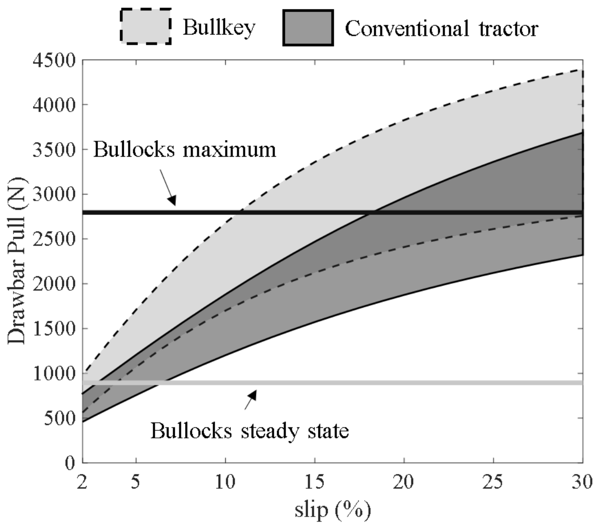

Fig. 9. A COMPARISON OF THE DRAWBAR PULL VERSUS SLIP PERFORMANCE IN WEAK TO STRONG AGRICULTURAL SOIL FOR A 500 KG HYPOTHETICAL IMPLEMENTATION OF A CONVENTIONAL TRACTOR AND BULLKEY (more details Table 2). The drawbar pull of a bullock pair has been added for reference. Soil data in Supplemental Material A.

Bullkey proof-of-physics prototype	
Base Vehicle	ROKON Scout [50]
Mass unballasted	192 kg
Mass supported by front wheel	82.5 kg
Mass supported by rear wheel	94 kg
Mass supported by outrigger	15 kg
Wheelbase	1.3 m
Rear ballast to rear axle	0.56 m
Front ballast to front axle	0.48 m
Turn radius (no lean)	1.4 m
Tire pressure	7 psi
Tire model	TITAN 489XT [51]
Tire size	12" rim, 8" x 25"
Tool used	0.3 m wide furrower

Table 3. BASIC PARAMETERS FOR BULLKEY PROTOTYPE.

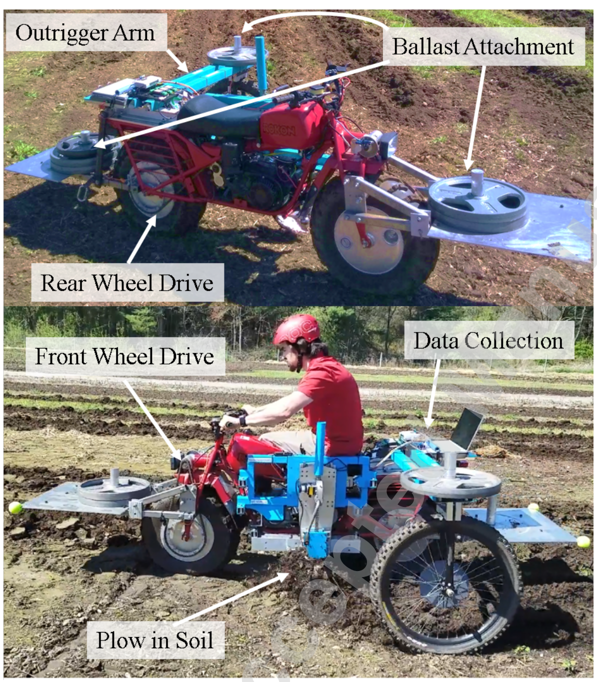

Fig. 10. BULLKEY PROTOTYPE VEHICLE HIGHLIGHTING THE IMPLEMENTATION OF DESIRABLE DESIGN FEATURES FOR A SMALL TRACTOR INTENDED TO REPLACE A PAIR OF BULLOCKS. These features include two inline drive wheels supporting almost the full vehicle weight, a manually controlled and centrally mounted heavy tillage tool, and motorcycle-type controls. Gym weights were used for ballast at the front, rear, and over the outrigger wheel.

wheeled motorcycle meant for heavy off-road duty. A removable frame (next to the driver in Fig. 10) was attached to the left side of the motorcycle to control the tillage tool position and record the forces it experienced. An outrigger arm extended parallel to the rear axle of the motorcycle, also on the left side (behind the driver's left in Fig. 10). The outrigger wheel's axle was in the same vertical plane as the rear drive wheel axle, making side-slip during slow speed turning negligible for the outrigger wheel. The parameters of the test vehicle are given in Table 3.

The prototype mass could be varied between 192 kg and 305 kg during testing. This mass range allowed testing of the tractor physics model at drawbar pull loads comparable to bullocks but without overloading the stock frame and transmission of the Rokon. The transmission began slipping at drawbar forces produced by the 305 kg tested configuration, and so the prototype could not be tested at the maximum expected production mass of 500 kg. The Rokon, which weighs only 98 kg, had crucial benefits not present in other heavier vehicles, including a unique inline drive wheel system and a frame designed for 20 cm wide tires. Building the Bullkey prototype with a commercially-available base vehicle allowed its most critical features to be evaluated without the time and financial burden of manufacturing an entirely new operator-safe vehicle. The prototype design incorporated the full proposed novel layout and was thus suitable for evaluating the drawbar pull force and overall functionality of the Bullkey concept. In combination with our prior work validating the traction model with published data for heavier commercial tractors [29], the prototype can be used to validate the physics model presented here, and so its predictions for other mass configurations should be accurate.

The prototype was designed to evaluate if the

Journal of Mechanical Design. Received November 30, 2019;
Accepted manuscript posted March 09, 2020. doi:10.1115/1.4046811

Fig. 11. CLOSE-UP VIEWS OF SENSOR INSTALLATION EXAMPLES. Views of prototype shown are (A) left-side, (B) outrigger wheel right side, and (C) rear axle left side

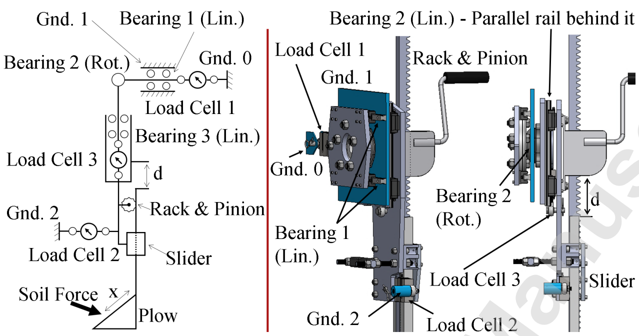

Fig. 12. MECHANICAL DIAGRAM AND CAD OF THE STRUCTURE USED TO MEASURE TILLAGE FORCES ON THE BULLKEY PROOF-OF-PHYSICS PROTOTYPE. Gnd. stands for ground (i.e. fixed to Bullkey's frame), Lin. for linear, and Rot. for rotary.

lightweight Bullkey tractor could achieve the predicted high drawbar pull force at tire slips recommended for plowing (15 to 25% [36]) and also have the ability to enter narrow inter-row spaces. Sensors were mounted to record tillage tool forces (equal and opposite to the tractor's generated drawbar pull when parallel to the tractor's pull), tillage tool force location, acceleration, and tire slip (Fig. 11). Tillage tool forces and their location were isolated for measurement by the attachment structure described in Fig. 12 and shown in Fig. 11A. The desired operating tillage tool depth was controlled by a Haacon 1524 rack and pinion jack (1524 SS by Haacon, Germany [52]) and recorded by a string potentiometer (CWP-S by CALT, China [53]) that attached to the pinion housing and the rack. The horizontal and vertical components of the tool force could be resolved from the three axial load cells (104-500 by DYLY, China [54]) that exactly constrained the motion of the tillage tool (Fig. 12). To exactly constrain each load cell, they were mounted in conjunction with a single degree-of-freedom linear (HSR15-600-A by Joomen, China [55]) or rotary (513267 Wheel Bearing and Hub by MOOG, USA [56]) bearing and placed to be the only load bearing elements in the force path of the loads they measured. These three load cells also allowed spatial resolution of the center of pressure for forces exerted on the tillage tool (along the x dimension in Fig. 12).

All three wheels were fitted with magnetic proximity sensors, with 10 evenly spaced magnets placed on each wheel (Fig. 11B). Tire slip can be calculated using the rotation of these senors, assuming that the idle outrigger wheel has near zero slip and can be used as the reference point for distance travelled. An accelerometer (ADXL335 by Adafruit, USA [57]) was placed at the rear axle to provide higher time resolution on vehicle speed and to assist in confirming short-term measurements from the outrigger wheel rotations (Fig. 11C). Sensor specifications are provided in Supplemental Material D.

5 Field testing and performance results

5.1 Field testing methods

Field tests were performed on a working farm in Massachusetts to validate the terramechanics model, investigate the traction performance of the Bullkey prototype, and obtain user feedback after operating the vehicle among actual growing crops. Traction performance tests were conducted at different tillage depths and different ballasting levels to alter the vehicle mass distribution from the base distribution specified in Sec. 4. Ballast on the front and rear ballast trays varied between 0 and 56 kg $\pm$0.5 kg, operator mass (of the author) during recorded tests was 79 kg $\pm$1 kg, and tire pressure was set to 41 kPa (6 PSI) $\pm$4 kPa. For each configuration, the tractor was driven in a straight line at about 1 m/s for 30 to 50 m with a 30 cm wide furrowing tool at a constant depth between 12 and 19 cm. Tool depth was set for each configuration to force tire slip to be near 20% – approximately the upper limit of what would be useful on a farm field and thus close to the vehicle's maximum practical drawbar pull [24] [23].

In addition to sensor data, field tests with the prototype vehicle provided an opportunity to gain valuable feedback on the usability of the proposed tractor design. Six local Massachusetts farmers observed the field tests and provided their feedback in a spoken survey. The survey was approved by MIT's Committe on Use of Humans as Experimental Subjects (COUHES). In addition to the drawbar pull tests on open farm fields, qualitative tests were performed by driving Bullkey between growing crop using a 15 cm wide sweep tillage point at 3 to 6 cm depth. A sweep is a thin "V" shaped tillage tool used cut weeds at their root between rows of growing crop during intercultivation.

The sensor data collected was processed to have a similar format as the initial simulations (Fig. 9). First, the col-

Journal of Mechanical Design. Received November 30, 2019;
Accepted manuscript posted March 09, 2020. doi:10.1115/1.4046811

lected time-force signals were passed through a 1 Hz low pass filter. This filtering frequency was selected because the 30 cm long tool travels at least three characteristic lengths every second. Then, the distance traveled by all wheels was calculated by summing the new distance traveled each time a wheel magnet (Fig. 11B) was detected, using linear interpolation to fill in the distance travelled for intervals between detections. The distance travelled between magnet detections is $2\pi/10 * R$, where $2\pi/10$ is the angular spacing between neighboring magnets in radians (there are 10 magnets per wheel) and R is the effective radius of the wheel (estimated by counting the number of wheel rotations to travel 30 m under the test conditions). The three (one per wheel) distance-travelled vectors were then processed through a 1 Hz low pass filter as well.

The drawbar pull versus tire slip binned data shown in Fig. 13 were generated by the following procedure: (1) The highest drive tire slip was selected at each timestamp and stored along with the drawbar pull measured at that timestamp to generate a slip vs. drawbar matrix. (2) This matrix was then rearranged so that all drawbar pull instances were assigned to the closest integer slip (i.e. all slip instances $\geq$13.5% and <14.5% were assigned to the 14% slip bin). (3) Finally, in each slip bin the average, minimum, and maximum drawbar pull were obtained and stored. As presented in Fig. 13, squares represent the average drawbar pull at that tire slip bin while the error bars represent that maximum and minimum drawbar pull recorded at that tire slip bin. Further details are presented in Supplemental Material E.

5.2 Field performance results

Figure 13 compares the drawbar pull performance for each of the Bullkey mass configurations tested against the steady state and the maximum pulling force of a bullock pair [25, 26, 49], as well as to the model-predicted performance for the soil conditions during the test and for the range of common farm soil conditions (provided in Supplemental Material D). The results validated that the physics model from Sec. 2 made predictions for the maximum drawbar pull that are sufficiently accurate to inform tractor design. The model average absolute error compared to experimental data was 7% at 15% slip, 9% at 20% slip, and 12% at 25% slip. The standard deviation for the absolute error was 4% at 15% slip, 5% at 20% slip, and 8% at 25% slip (full results in Supplemental Material B). All tested configurations comfortably surpassed the steady-state pulling of bullocks. The maximum drawbar pull for the 305 kg Bullkey configuration, despite being limited by the test soil not being at the upper limit of strength for agricultural soils, was near to the maximum pulling force for a pair bullocks. More importantly, given the demonstrated accuracy of the model, it is expected that a heavier Bullkey (up to 500 kg) would be able to match or exceed the maximum pulling force of a bullock pair for any common agricultural soil condition, as was predicted in Fig. 9. This cannot be matched by a conventional tractor layout of the same mass.

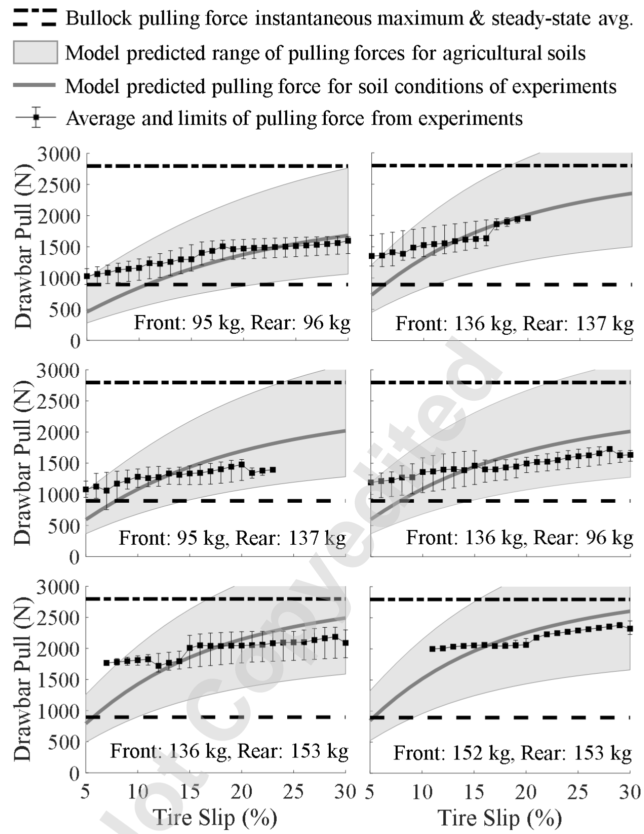

Fig. 13. EXAMPLES OF MEASURED FORCES FOR PROTOTYPE CONFIGURATIONS TESTED. Indicated in each plot are the masses supported by the Bullkey prototype's front and rear wheels when static and with no driver on board. The masses were adjusted by adding and removing ballast.

5.3 User feedback

On-site farmers who observed the Bullkey prototype during field tests said that the vehicle had valuable and unique benefits for small farmers. Farmers appreciated the ease with which the tool could be observed during tillage and the tall height of the outrigger arm, which allowed the vehicle to easily straddle crop rows. They also commented positively on the Bullkey prototype's ability to plough deeper than they would have expected from such a small vehicle. Farmers were initially concerned that the tillage tool's lateral offset from the drive tires might cause Bullkey to veer off-track – this concern was allayed when they watched Bullkey maneuver and saw that it was easy to drive the vehicle in a straight line under all conditions. The farmers also had some suggestions for improving the vehicle. They suggested having a mount for low drawbar force tools, like those used during intercultivation, set up behind the rear axle and in line with the drive wheels in order to provide better access to narrow rows while crops are growing.

6 Discussion

The Bullkey prototype's measured maximum drawbar pull matched well to model predictions in both trends and absolute values. This showed that the model is a useful tool to evaluate potential tractor designs for traction performance and identify promising design directions. The average absolute error of the model at high slips (when maximum drawbar pull occurs) was generally less than 10%. The model's performance and its parametric, physics-based foundation make it useful for exploring a large design space of previously unrealized tractor designs. These capabilities make it a powerful tool for identifying and establishing the Bullkey design.

The prototype's field performance showed that the Bullkey design satisfied the outlined user needs for an easy to use, highly maneuverable lightweight vehicle with high drawbar pull capability for a low mass device. Bullkey was able to straddle rows of growing crops on the field because of its configuration of inline drive wheels with an outrigger arm. This enabled Bullkey to operate in narrow inter-row spaces like bullocks do – something that is not possible with conventional tractors. Bullkey generated more drawbar pull per unit mass than conventional tractors with rear drive wheels and rear mounted tools – this is significant because mass is correlated approximately linearly with cost (Fig. 2). Bullkey's performance on the field therefore suggests that a production-version of the tractor could be sold at a lower cost for a given drawbar pull capacity than available tractors, enabling the distribution of a tractor that can compete with the maximum pulling force and the purchase price of bullocks.

Bullkey was comfortable to operate after some adjustments were made. A 20 kg ballast was added to the outrigger wheel after early field tests and mitigated the risk of the tractor rolling over sideways. During instrumented testing the operator would sit side saddle - a remnant habit from an earlier, taller version of the tillage tool attachment mechanism shown in Fig 12 - which shifted the overall center of mass away from the outrigger wheel and decreased stability. During later driving the operator sat as is conventional, straddling the motorcycle frame and the tillage tool mounting frame, which was an improvement in comfort. The front drive wheel never became unweighted during tests with heavy drawbar loads (a common occurrence with conventional tractors [58–60]), which makes Bullkey safer near its traction limits than conventional tractors.

The proof-of-physics Bullkey prototype allowed testing to find its drawbar pull at slips relevant to tillage and near its traction limits (15 to 25% tire slip). A limitation of the presented work is that the accuracy of the modeled drawbar pull drops for slips under 10% (Fig. 13). It is possible that at lower slip the assumed soil deformation mechanics are less applicable, or that the vehicle was at least partially relying on other methods of forward propulsion during low slips (like its inertia when slowing down). These errors could have been accentuated by the experimental methods, which focused on finding the tractor's maximum drawbar pull at high tire slips and not on generating steady drawbar pull at low tire slips. Future work could include experiments at constant low tire slips, to better capture the performance of the model in those conditions and identify strategies for model improvements. The model is usable for its design purposes in this paper, which is to estimate the maximum drawbar pull of multiple designs, which occurs at high tire slips.

The Bullkey prototype was usable for farming operations that could be performed with tillage tools mounted centrally on the vehicle (like plowing and furrowing). To add flexibility, a future prototype could allow low drawbar force farming tools via conventional mounting points behind the tractor, like a three point hitch and a pin or ball hitch. Future work could also allow for ballast to be added without extending the overall length of the vehicle. A key next step is to discuss the Bullkey vehicle with small Indian farmers – the target users – to solicit feedback on the vehicle design and usability. In these discussions, farmers could also be asked if they might use Bullkey (with some attachments removed) as a conventional two-wheel motorcycle for personal transportation. If Bullkey is viable as a two-wheeler, it could replace both a pair of bullocks and a motorcycle for farmers, further increasing its value proposition.

7 Conclusions

The presented tractor design, Bullkey, is novel in its high potential to concurrently match bullocks' sales price, pulling strength, and unique ability to access a field with growing crop, while also offering farmers major conventional tractor benefits like increased productivity, lower maintenance costs, and improved comfort. This allows Bullkey to fulfill the unique needs of small farmers in India, which are not currently being met by commercially available tractors.

Bullkey has inline drive-wheels that support the majority of the its mass, a crop clearance similar to a bullock team yoke, and a centrally located tillage tool attachment. Inline drive enabled improved traction, reduced soil compaction, and operating in narrow inter-row spaces between growing crop. Central tool attachment increased traction and improved safety while also facilitating the operator maintaining control over the direction they are driving as well as the tillage operation being performed. These beneficial design features were identified by combining insights from a physics-based traction model and farmer interviews. The traction performance predicted by the model was validated by field testing an instrumented prototype of Bullkey.

Replacing bullocks with a suitable farm tractor, such as the Bullkey design proposed here, could increase farmer income by 20% and reduce their recurring expenses by 60%. Farmer income could increase because of higher crop yields from more precise and timely farm operations. Recurring expenses would be reduced because tractor maintenance is much lower over the course of a year than the daily feed and care costs of bullocks. The findings presented in this paper will be useful to engineers developing lightweight, high drawbar pull vehicles and/or vehicles that are well suited to in-field use by small farmers in emerging markets.

Acknowledgements

The authors would like to thank Mahindra Tractors for sponsoring this work, as well as their technical and logistical support. Thank you also to the MIT Tata Center for sponsoring this work. Thank you to Gwyndaf Jones, Dan Dorsch, Shane Pratt , Susan Amrose, Julia Sokol, and Brett Johnson for their help with field tests and reviewing this manuscript.

Journal of Mechanical Design. Received November 30, 2019;
Accepted manuscript posted March 09, 2020. doi:10.1115/1.4046811

References

[1] Hazell, P. B. R., 2015. "Is small farm-led development still a relevant strategy for africa and asia?". *Oxford Scholarship*.

[2] Yadav, S., and Lohan, S. K., 2006. "Tractor and implement ownership and utilization of haryana". *Agricultural Mechanization in Asia, Africa AND Latin America,* ***37***.

[3] Mehta, C., Chandel, N., Jena, P., and Jha, A., 2019. "Indian agriculture counting on farm mechanization". *Agricultural Mechanization in Asia, Africa AND Latin America,* ***50***.

[4] of Agriculture for Government of India, M., 2019. "Agriculture census 2015-2016". *Agriculture Census Division*.

[5] Lowder, S., Skoet, J., and Singh, S., 2014. "What do we really know about the number and distribution of family farms worldwide? background paper for the state of food and agriculture". *ESA Paper No. 14-02. Rome FAO*.

[6] Indian Agrigultural Ministry, 2013. "Presentation on farm mechanization before parliamentary consultative committee".

[7] Engineers at Mahindra and Mahindra Co. "Conversations with mahindra and mahindra tractor company on tractor adoption in india. met multiple times from 2014 to jan. 2019.".

[8] Foster, A., and Rosenzweig, M. R., 2010. "Barriers to farm profitability in india: Mechanization, scale and credit markets.". *World Bank Resources*.

[9] FAO (Food and Agricultural Organization), 2013. "Mechanization for rural development: A review of patterns and progress from around the world". *Integrated Crop Management*.

[10] NSL Srivastava, 2006. "Farm power sources, their availability and future requirements to sustain agricultural production". *Indian Council of Agricultural Research*.

[11] G Spoor and R Carillon and L Bournas and EH Brown, "1987. *The Impact of Mechanization*. John Wiley and Sons Ltd., Chichester, New York.

[12] USA Census Bureau, 1950. "Agriculture 1950: Changes in agriculture, 1900 to 1950". Web PDF.

[13] Lankenau, G. F. D., Daigle, L., Ihns, S. H., Koch, E., Saadi, J., Tornes, P., Wu, J. M., and Amos G. Winter, V., 2019. "Design of a human-powered roll stabilization attachment for utilitarian two-wheeled vehicles". *ASME IDETC*. Anaheim, CA.

[14] Singh, S., 2009. "Agricultural machinery industry in india a study of grwoth, market strategy, and business strategies". *Centre for Management in Agriculture. Indian Institute of Management Ahmedabad*.

[15] Engineers at Mahindra and Mahindra Co. "Conversations with farmers and researchers in india on tractor adoption. met multiple times from 2014 to sept. 2019.".

[16] Department of Agriculture, Cooperation and Farmer Welfare, 2019. "Annual report 2017 to 2018". *Government of India Ministry of Agriculture Farmers Welfare*.

[17] Food, Advisory, A. S., Research (FASAR), Y. B., and at OAV German Asia-Pacific Business Association (GAA), G. A. A., 2016. "Farm mechanization in india. the custom hiring perspective". *Indian Ministry of Agriculture and Farmers Welfare*.

[18] Prabu M J, 2010. "A tilting cart offers relief to animals and workers in the field.". *The Hindu*. April 21.

[19] Philip, A J, 2017. "Cow protection". *Indian Currents*. April 10.

[20] Damodaran, Harish, 2017. "What it might cost to save gauvansh countrywide.". *The Indian Express*. April 24.

[21] H. Goel, V. Kumar, 2013. "Automobiles, sixth gear". *Kotak Institutional Equities*, Jan.

[22] Arelekatti, V. N. M., Björkdal, D. H., Graves, C. W., Wong, A., Mkrtchyan, A., and V, A. G. W., 2014. "Proof-of-concept evaluation of a low-cost and lowweight tractor for small-scale farms". In ASME IDETC 2014.

[23] Brixius, W., 1987. "Traction prediction equations for bias ply tires.". *ASAE Paper*.

[24] Zoz, F. M., and Grisso, R. D., 2003. "Traction and tractor performance". In Agricultural Equipment Technology Conference, pp. 1–47.

[25] Goe, M. R., and McDowell, R. E., 1980. "Animal traction guidelines for utilization". *Cornell International Agriculture Mimeograph*.

[26] Watson, P. R., 1981. "Animal traction". *Peace Corps. by TransCentury Corporation*.

[27] Reddy, B. S., Srinivas, I., Adake, R. V., Thyagraj, C., Reddy, K. S., and Rao, C. S., 2015. "Small farm mechanization technologies and transfer strategies". *Indian Farming,* ***65***.

[28] of Food, I. C., and Agriculture, 2017. "Farm mechanization national round table conference".

[29] Guillermo F. Diaz Lankenau and Amos G. Winter V, 2018. "An engineering review of the farm tractor's evolution to a dominant design". *ASME Journal of Mechanical Design*. doi:10.1115/DETC2018-86285.

[30] J.Y. Wong and A. Reece, 1967. "Prediction of rigid wheel performance based on the analysis of soil-wheel stresses part i. performance of driven rigid wheels". *Journal of Terramechanics*, pp. 81–98.

[31] Bekker, M. G., 1956. *Theory of Land Locomotion*. University of Michigan Press.

[32] Senatore, C., 2010. "Prediction of mobility, handling, and tractive efficiency of wheeled off-road vehicles". PhD dissertation, Virginia Polytechnic Institute and State University, Department of Mechanical Engineering.

[33] Holm, I., 1969. "Multi-pass behaviour of pneumatic tires". *Journal of Terramechanics*, pp. 47–71.

[34] Ghotbi, B., Gonzàlez, F., Kövecses, J., and Angeles, J., 2015. "Effect of multi-pass on the mobility of wheeled robots on soft terrain". In ECCOMAS Thematic Conference on Multibody Dynamics.

[35] Wong, J., 2010. *Terramechanics and Off-Road Vehicle Engineering*. Elsevier, Oxford, UK.

Journal of Mechanical Design. Received November 30, 2019;
Accepted manuscript posted March 09, 2020. doi:10.1115/1.4046811

[36] Smith and Grisso, 1990. "Using tillage horsepower more efficiently: Selecting speed, slip and ballast". In Conservation Tillage Proceeding 9:79-81.

[37] Battiato, A., Diserens, E., and Sartori, L., 2013. "Traction performance simulation for mechanical front wheel drive tractors: towards a practical computer tool". *Journal of Agricultural Engineering*.

[38] Battiato, A., Diserens, E., and Sartori, L., 2017. "Tractor traction performance simulation on differently textured soils and validation: a basic study to make traction and energy requirements accessible to the practice". *Soil and Tillage Research*.

[39] Shibly, H., 2017. "Analysis of the effect of soft soil's parameters change on planetary vehicles' dynamic response". *Journal of Automation, Mobile Robotics and Intelligent Systems,* ***11***.

[40] Antille, D. L., Bennett, J. M., and Jensen, T. A., 2016. "Soil compaction and controlled traffic considerations in australian cotton-farming systems". *Crop and Pasture Science*.

[41] de Souza, G. S., de Souza, Z. M., da Silva, R. B., Barbosa, R. S., and Araùjo, F. S., 2014. "Effects of traffic control on the soil physical quality and the cultivation of sugarcane". *Revista Brasileira de Ciência do Solo*.

[42] Onal, I., 2012. "Controlled traffic and widespan tractors". *Tarim Makinalari Bilimi Dergisi (Journal of Agricultural Machinery Science)*.

[43] Chamen, T., 2014. "Controlled traffic farming – from worldwide research to adoption in europe and its future prospects". In International Conference of Agricultural Engineering.

[44] Oden, D. S., 2006. "Harvest of hazards the farm safety movement". *PhD thesis at Iowa State University*.

[45] Farm, Safety, R., and of British Columbia, H. A., 2016. "Agricultural equipment safety". *SAFE Work Manitoba Communicatios*.

[46] NAG, P. K., and NAG, A., 2004. "Drudgery, accidents and injuries in indian agriculture". *Journal of Industrial Health,* ***42***.

[47] Mahindra Tractors, 2019. Yuvraj nxt 215. https://www.mahindratractor.com.

[48] Aruna Pal and P.N. Chatterjee, 2013. "Field level study on the buffalo bullock, an excellent draught animal". *Buffalo Bulletin,* ***32***.

[49] Research and Experimental Centre for Tropical Mechanical Agricultural Equipment, 1972. "The employment of draught animals in agriculture". *Food and Agriculture Organization of the United Nations*.

[50] Rokon International Inc., 2019. Company website with details on vehicles. https://www.rokon.com/bikes/scout.

[51] Titan Tire, 2019. 489 xt, Oct. http://www.titantirestore.com.

[52] Haacon Lifting Technology, 2019. Model 1524 pinion and rack. https://www.haacon.com.

[53] CALT 500mm Measure Range 0-5Kohm Draw Wire Potentiometer, 2019. Website with details on sensor. https://www.amazon.com/dp/B01FHDL81Y.

[54] China Enconder, 2019. Pull pressure force sensor s-type load cell 300kg 500kg 1.5t for concrete mixing station batching scale hopper scale pressure testing machine (500kg), Oct. https://www.amazon.com/dp/B01HHO5RNQ.

[55] Joomen, 2019. Joomen cnc set 15-600mm 2x linear guideway rail 4x square type carriage bearing block, Oct. https://www.amazon.com/dp/B01CMG0OMS.

[56] MOOG Suspension Parts, 2019. moog-513267 | front wheel bearing hub assembly | acura mdx 4wd, Oct. https://www.moog-suspension-parts.com.

[57] Adafruit, 2019. Adxl335 - 5v ready triple-axis accelerometer (+-3g analog out), Oct. https://www.adafruit.com/product/163.

[58] Abubakar, M. S., Ahmad, D., and Akande, F. B., 2010. "A review of farm tractor overturning accidents and safety". *Petranika Journal of Science and Technology*.

[59] Demsar, I., BERNIK, R., and Duhovnik, J. "A mathematical model and numerical simulation of the static stability of a tractor". *Agric. conspec. sci. Vol. 77 (2012) No. 3*.

[60] Smith, D. W. "Safe tractor operation: Rollover prevention". *Texas Agricultural and Mechanical University. AgriLife Extension. 2005*.

[61] Mital, M., and Gawade, R., 2019. Tractor price, new tractors, buy and sell used tractors, Oct. https://tractorguru.in/.

[62] Tractor Junction, 2019. New tractors price in india, top tractor brands, specs, photos, reviews and videos, Oct. https://www.tractorjunction.com/tractors.

[63] Tacuna Systems, 2019. Load cell amplifier strain gauge amplifier, Oct. https://tacunasystems.com.

[64] Automation Direct, 2019. Mafm1-a0-1h, Oct. https://www.automationdirect.com.

[65] DataQ Instruments, 2019. Di-2108 8-channel high speed usb data acquisition system, Oct. https://www.dataq.com/products/di-2108/.

Journal of Mechanical Design. Received November 30, 2019;
Accepted manuscript posted March 09, 2020. doi:10.1115/1.4046811

Supplemental Material is provided next

Journal of Mechanical Design. Received November 30, 2019;
Accepted manuscript posted March 09, 2020. doi:10.1115/1.4046811

Supplemental Material A: Costs for farming with bullocks or conventional tractors in Indian small farms

Aspect	Variable	Tractor	Bullock Pair	Units
Capital Cost	C	200000	80000	INR
Principal on Loan	P	20	N/A	% of C
Interest on Loan	I	16	N/A	% of C
Annual operating cost 1 hectare	O	12500	60000	INR/year
Time before replacement	T	10	13	years
Resale value when replaced	R	50000	0	INR
Time elapsed	t	15	15	years

Table 4. Breakdown of costs to an Indian farmer for purchasing a tractor (financed and upfront) or a pair of bullocks. [7, 15, 18–21]

To calculate the costs of ownership for 15 years, the equations below were used with values from Table 4. Yearly maintenance costs were assumed to remain constant through time for both tractor and animals. At the end of their useful life as draft animals, bullocks cannot be sold in India [20] but reasonably maintained tractors can be sold for at least 25% of their original value after 10 years [21]. The Bullkey tractor is assumed to have equivalent ownership costs to a conventional tractor but with an estimated capital cost of 100,000 INR and a corresponding resale price of 25,000 INR after 10 years. The capital cost for Bullkey is a target as mentioned by farmers, not a final price.

Total ownership costs for tractor or bullock pair bought up front:

ownership cost total for 15 years = $tO + 2C - R$

Total ownership costs for tractor financed:

ownership cost total for 15 years= $tO + 2C - R + 2(C - P)I$

Journal of Mechanical Design. Received November 30, 2019;
Accepted manuscript posted March 09, 2020. doi:10.1115/1.4046811

Supplemental Material B: Average drawbar pull results compared to model predictions

		Avg. Drawbar Pull (N) and Model Error (%) at Varying Tire Slip											
Vehicle Mass		**10% slip**			**15% slip**			**20% slip**			**25% slip**		
Front	**Rear**	actual	model	error	actual	model	error	actual	model	error	actual	model	error
95kg	96kg	1162	849	-26.9	1300	1161	-10.7	1472	1391	-5.5	1513	1564	3.3
95kg	96kg	1297	849	-34.5	1333	1161	-12.9	1350	1391	-3	1479	1564	5.7
95kg	137kg	1281	1086	-15.2	1313	1441	9.7	1478	1697	14.8	1425	1882	32
136kg	96kg	1360	1096	-19.4	1461	1448	-0.9	1495	1698	13.6	1612	1878	16.5
136kg	96kg	1324	1096	-17.2	1516	1448	-4.4	1509	1698	12.5	1616	1878	16.2
136kg	137kg	1436	1326	-7.7	1624	1735	-6.8	1688	2015	19.4	N/A	2211	N/A
136kg	137kg	1526	1326	-13.26	1623	1735	-6.8	1955	2015	3.1	N/A	2211	N/A
136kg	153kg	N/A	1431	N/A	1989	1923	-3.3	2026	2148	6	2158	2347	8.8
136kg	153kg	1825	1431	-21.5	2009	1923	-4.3	2056	2148	4.5	2141	2347	9.6
152kg	153kg	1999	1653	-17.3	2056	1968	-4.3	2065	2262	9.5	2317	2463	6.3
152kg	153kg	1568	1653	5.4	1694	1968	16.2	2092	2262	8.1	2110	2463	16.7

Table 5. SUMMARY OF RESULTS FROM FIELD TEST EXPERIMENTS COMPARED TO MODEL PREDICTIONS. For reference, 64% drawbar pull to mass ratio for all configuration masses is 191 kg : 1199 N, 232 kg : 1456 N, 273 kg : 1714 N, 289 kg : 1814 N, 305 kg : 1914 N

Journal of Mechanical Design. Received November 30, 2019;
Accepted manuscript posted March 09, 2020. doi:10.1115/1.4046811

Supplemental Material C: Common Indian Tractor Sale Prices and Size

Make	Model	Mass (kg)	Engine Power (hp)	Min. Price (1000 INR)
Jyoti	Sanedo	450	12	120
Madhav Agro	DI 510	515	10	215
Blue Chemp Agro	MS-120	520	12	170
VST Shakti	MT 180 D JAI 2W	645	19	295
VSt Shakti	MT 180D	645	18.5	295
Kubota	NeoStar B2741 4WD	650	27	545
VST Shakti	MT 224 1D AJAI 4WD	740	22	356
Captain	120 DI	780	15	250
Mahindra	Yuvraj 215 NXT	780	15	200
VST Shakti	MT 171 DI Samraat	800	13	275
Sonalika	GT 20 RX	820	20	300
Sonalika	GT 22	850	22	343
Swaraj	717	850	15	260
Captain	200 DI	885	17	265
Captain	200 DI 4WD	940	17	310
Farmtrac	Atom 26	990	26	480
John Deere	3028 E	1070	28	565
John Deere	3036 E	1295	36	740
Farmtrac	60	1400	50	630
TAFE	30 DI Orchard Plus	1400	30	420
Swaraj	724 XM Orchard	1430	25	395
Massey Ferguson	1035 dI Maha Shakti	1700	39	495
Eicher	364 Super DI	1710	32	471
Massey Ferguson	1035 DI	1713	35	490
Massey Ferguson	1134 MAHA SHAKTI	1720	34	470
Eicher	242	1735	25	355
John Deere	5005	1750	33	470
John Deere	5039 D PowerPro	1760	41	570
New Holland	3032	1760	35	520
Mahindra	275 ECO	1760	35	455
John Deere	5042 D PowerPro	1810	44	625
Powertrac	439 Plus	1850	41	530
Kubota	MU4501	1850	45	715
John Deere	5205	1870	48	690
Swaraj	735 FE	1895	39	550
Powertrac	ALT 4000	1900	41	530
Farmtrac	Champion 39	1940	39	490
Massey Ferguson	7250 Power	1950	47	620
Massey Ferguson	241 4WD	1950	42	620
John Deere	5050 D - 4WD	1975	50	800
Eicher	371 Super Power	1995	37	475
John Deere	5045 D - 4WD	2010	45	770
Mahindra	475 DI	2019	42	545
Swaraj	855 FE	2020	52	710
Mahindra	Yuvo 575 DI	2020	45	628
Mahindra	Yuvo 415 DI	2020	40	570
Eicher	380 Super DI	2045	40	530
New Holland	3600 Tx Heritage Edition	2055	47	650
New Holland	3630 TX Plus	2080	55	725
Mahindra	585 DI Power Plus BP	2100	50	600
John Deere	5310	2110	55	789
Digitrac	PP 43i	2140	47	585

Journal of Mechanical Design. Received November 30, 2019;
Accepted manuscript posted March 09, 2020. doi:10.1115/1.4046811

Powertrac	Euro 50	2170	50	610
Swaraj	963 FE	2200	60	790
Kubota	MU5501	2200	55	870
Farmtrac	45 EPI Classic Pro	2245	48	590
New Holland	Excel 4710	2255	47	660
John Deere	5405 GearPro	2280	63	850
Digitrac	PP 46i	2470	50	630
Sonalika	WT 60 SIKANDER	2520	60	790

Table 6: Common tractors sold in India with their mass, engine power, and lowest typical sale price. The tractors are sorted by mass. Data collected by authors from online tractor sale websites [61, 62].

Journal of Mechanical Design. Received November 30, 2019;
Accepted manuscript posted March 09, 2020. doi:10.1115/1.4046811

Supplemental Material D: Soil properties and sensors used for tests

	Soil Type		
Property	**Weak**	**Strong**	**Actual**
n	1.1	0.79	1
Cohesion (kPa)	0.6	20	3.3
Friction angle (deg)	28	18	33.7
k'_c (kN/m^2)	0.990	2354	74.6
k'_ϕ (kN/m^3)	1528	-4130	2080
Bulk density (kg/m^3)	1310	1580	1557

Table 7. Soil properties used to generate plots. Soils properties for limit conditions are the upper and lower strength limits of soils published soil traction parameter tables [35] [38]. Actual soil strength for field tests is from matching soil type, cone penetromenter data, and soil moisture data from field test to the most appropriate soil parameters in [35].

String Potentiometer (Tool Position)	
Sensor [53]	CALT CWP-S
String Length	500 mm
Resistance Range	0-500 kOhm
Force (Tool Loads)	
Sensor [54]	DYLY 104-500
Load Range	±500 kg
Sensitivity	2.0 ± 0.05 mV/V
Non-Linearity	±0.03≤%F·S
Hysteresis	±0.03≤%F·S
Amplifier [63]	Tacuna EMBSGB200
Amplification	1&2 @550x, 3 @220x
Magnetic Proximity (Wheel Rotations)	
Sensor [64]	MAFM1-A0-1H
Switching Freq.	5 kHz
Magnets	Neodymium 10x3 mm
Magnets per rotation	10
sensor to magnet	5 mm
Acceleration (Vehicle Motion)	
Sensor [57]	Adafruit ADXL335
Range	±3 g
Bandwidth	50 Hz
Data Acquisition (All Sensors)	
Device [65]	DATAQ DI2108
Resolution	16 bit
Capture Rate	10 kHz

Table 8. Overview of electronics used for data collection.

Journal of Mechanical Design. Received November 30, 2019;
Accepted manuscript posted March 09, 2020. doi:10.1115/1.4046811

Supplemental Material E: Data processing from experiments

Processing of the collected sensor data was performed in MATLAB. First, the drawbar force components were calculated at every instant. To define the drawbar components and their point of application, soil force D and center-of-pressure position x are calculated from Eqns 9, 10 and 11.

$$D = \sqrt{(R_A - R_B)^2 + R_C^2} \tag{9}$$

$$\alpha = tan^{-1}\left(\frac{R_C}{R_A - R_B}\right) \tag{10}$$

$$x = \frac{-R_A * (d + l + q) + R_B * (d + 2l + q)}{(R_A - R_B * sin(\psi) - R_C * cos(\psi)} \tag{11}$$

Where, in reference to Figs. 12 and 3, R_A is the tension force on Load Cell 1, R_B is the tension force on Load Cell 2, R_C is the tension force on Load Cell 3, l is the vertical distance from Load Cell 1 to Load Cell 2, q is the vertical vertical distance from Load Cell 2 to the origin of distance x when d = 0, d is the distance the tool jack has been lowered from its storage position, and γ is the angle of attack for the plow.

After the data was loaded into MATLAB, the resulting time-force signals were processed through a 1 Hz low pass filter, selected at this frequency because 1 second is the time it takes the tool to travel three characteristic lengths. Then, the distance traveled by all wheels was calculated by summing the new distance traveled each time a magnet was detected ($2\pi/10 * R_{effective}$) and using linear interpolation to fill in gaps when no magnet was detected. The three (one per wheel) distance-travelled vectors were then processed through another 1 Hz low pass filter. The highest drive tire slip was selected at each instant, along with its corresponding drawbar pull. This matrix was then rearranged so that all drawbar pull instances were assigned to the closest integer slip (i.e. all slip instances between 13.5% and 14.5% were assigned to the 14% slip bin). Finally, the drawbar pull values in each slip bin were averaged.